

Increasing Capacity of Multi-Cell Cooperative Cellular Networks with Nested Deployment

Qiong Wu[†] and Qilian Liang^{†‡}

[†]Department of Electrical Engineering, University of Texas at Arlington, Arlington, TX 76019-0016 USA

[‡]College of Electronic and Communication Engineering, Tianjin Normal University, Tianjin 300387 China

Email: qiong.wu@mavs.uta.edu, liang@uta.edu

Abstract—This paper proposes a novel deployment for multi-cell cooperative cellular networks based on the two-dimensional (2D) nested co-array, and analyzes its sum-rate capacity and spectrum efficiency. The system model is based on the traditional hexagonal cellular array, in which each hexagon represents a marocell. We take advantage of the invariance in the difference co-array so that the 2D nested array is able to calculate all elements in the covariance matrix of channel fading coefficients. Based on this premise, we demonstrate that the derivation procedure of average sum-rate capacity for the cooperative cellular networks is still valid for the nested distributed base stations (BSs) in the non-fading and Rayleigh fading channels. In numeric simulations, the derived formulas are consistent with the results from previous references. More importantly, given the same number of BSs, the proposed distribution significantly increases the sum-rate capacity of the system.

I. INTRODUCTION

Cellular networks are important parts of wireless communication systems. As the number of macro-cellular BSs reaching 50 million worldwide by 2015 [1], it has driven intensive research to fully utilized these facilities catering the growing demand for high-data rate services.

There are quite a few works [2] indicating that sophisticated cooperations among multiple BSs could achieve enormous gain over the lone-BS model. By increasing the level of collaboration, the multiple BSs are regarded as a distributed antenna array, and the multi-input multi-output (MIMO) techniques can be used to increase capacity, decrease interference, and perform distributed beamforming. Specifically, the downlink channel is commonly considered as a Gaussian noise plus interference broadcast channel (BC), and applied single-user detection because of the complexity and power constraints of the mobile receivers. The uplink channel is usually modeled as a multiple-access channel (MAC), because there are less restrictive limitations at the BSs, and the received signals are joint processed for the system enhancement [3].

For the uplink channel, an early study by Wyner [4] presented an analytically tractable model, in which the cells were ordered in an infinite linear vector or 2D hexagonal matrix. It derived optimal throughput and linear minimum mean-square error for non-fading channels. These results were extended to flat-fading channels in [5], where the fading was observed to increase the throughput under certain circumstances.

For the downlink channel, the sum-rate of a multiple-antenna cellular system was addressed with power constraints

for each BS in [6] by taking advantage of the duality principle between the BC and MAC [7]. “Dirty paper coding” (DPC) principle [8] was also applied to eliminate the effect of uncorrelated additive interference. The corresponding achievable rate and improvements of spectrum efficiency and sum-rate capacity for fading channel were reported in [9]–[11].

However, on the other hand, there are several inherent problems. First of all, because of the limitation of backhaul links, it is impossible to recruit an arbitrary number of BSs in order to achieve enormous spectrum efficiency gains [12]. Besides, if the cooperative network is modeled as a cluster and put into a larger system that one cluster is adjacent to the others, the out-of-cluster interferences would hinder further improvement as the per-cluster transmit power increases [2].

In this paper, a novel nested-distributed network is introduced to advance the research on joint multi-cell processing. It is also the first literature analyzing the cellular system with the nested-distributed BSs from the information-theoretic point of view. The nested array is firstly introduced to perform array processing with increased degrees of freedom using much fewer physical sensors [13]. The paper [14] generalizes this concept to the multiple dimensions, and provides the optimal structure to maximize the number of elements in the virtual co-array, as well as derives closed-form expressions for the sensor locations and the exact degrees of freedom obtainable from the proposed array as a function of the total number of the sensors.

The paper is organized as follows. Section II introduces the theoretical backgrounds for both 2D nested array and sum-rate capacity of cooperative multi-cell processing, as well as the basic assumptions for the network model. Section III derives the invariance of the difference co-array in order to obtain the capacity of nested distributed network. In Section IV, the numeric results are provided to validate the proposed propositions. Finally, we summarize the paper in Section V, and provide the directions for further research.

II. PRELIMINARY AND MODEL DESCRIPTION

A. 2D Nested Co-Array

The first two concepts relate with multidimensional lattice, which is extensively used to represent the nest co-array.

Definition 1 (Fundamental Parallelepiped (FPD) [14]). *The FPD of $\mathbf{V} \in \mathcal{C}^{D \times D}$ in D dimensions FPD(\mathbf{V}) is defined as*

the set of all vectors of the form

$$\{\mathbf{V}\mathbf{x}, \mathbf{x} \in [0, 1)^D\}.$$

Visually, $FPD(\mathbf{V})$ consist of all points contained in the parallelepiped whose sides are given by the two column vectors of \mathbf{V} . Its volume is given by $|\det(\mathbf{V})|$ and the density of the lattice points is the inverse of its volume.

Definition 2 (Shifted FDP (SFPD)). For arbitrary integers k_1 and k_2 , the SFPD is defined as the $FPD(\mathbf{N}^{(s)})$ shifted by the vector $[k_1, k_2]^T$, which is

$$SFPD(\mathbf{N}^{(s)}, k_1, k_2) \triangleq \left\{ \mathbf{N}^{(s)}([k_1, k_2]^T - \mathbf{x}), \mathbf{x} \in [0, 1)^2 \right\}.$$

The following definition provides one of the configuration for nested co-array deployments, and the consecutive theorem guarantees that this Definition 3 satisfies the requirements of both FPD and SFPD.

Definition 3 (2D Nested Co-Array). A two dimensional nested array is described by a 2×2 non-singular matrix $\mathbf{N}^{(d)}$, an integer matrix \mathbf{P} and integers $N^{(s)}$, $N^{(d)} = \det(\mathbf{P})$, and satisfying

- 1) A dense array with $N^{(d)} = \det(\mathbf{P})$ elements on lattice generated by $\mathbf{N}^{(d)}$, with sensor locations given by $\{\mathbf{N}^{(d)}\mathbf{n}^{(d)}, \mathbf{n}^{(d)} \in FPD(\mathbf{P})\}$.
- 2) A sparse array $\mathbf{N}^{(s)} = \mathbf{N}^{(d)}\mathbf{P}$, with sensor locations given by $\mathbf{N}^{(s)}[k_1, k_2]^T$ with $0 \leq k_1 \leq N_1^{(s)} - 1$, $0 \leq k_2 \leq N_2^{(s)} - 1$.
- 3) $N_1^{(d)}N_2^{(d)} = N^{(d)}$ and $N_1^{(s)}N_2^{(s)} = N^{(s)}$, where $N_1^{(d)}$ and $N_2^{(d)}$ are the number of rows and columns for the dense array, and $N_1^{(s)}$ and $N_2^{(s)}$ are corresponding numbers for the sparse array.

Theorem 1. Consider two nonsingular 2×2 matrices $\mathbf{N}^{(s)}$ and $\mathbf{N}^{(d)}$ related by an integer matrix \mathbf{P} as $\mathbf{N}^{(s)} = \mathbf{N}^{(d)}\mathbf{P}$.

- 1) Any point on $\mathbf{N}^{(d)}\mathbf{n}$ on the lattice $\mathbf{N}^{(d)}$ can be expressed as $\mathbf{N}^{(d)}\mathbf{n} = \mathbf{N}^{(s)}\mathbf{n}^{(s)} - \mathbf{N}^{(d)}\mathbf{n}^{(d)}$ where $\mathbf{n}^{(s)}$ is an integer vector and $\mathbf{n}^{(d)} \in FPD(\mathbf{P})$.
- 2) All points within $SFPD(\mathbf{N}^{(s)}, k_1, k_2)$ can be generated by the differences $\{\mathbf{N}^{(s)}[k_1, k_2]^T - \mathbf{N}^{(d)}\mathbf{n}^{(d)}, \mathbf{n}^{(d)} \in FPD(\mathbf{P})\}$.

B. Sum-Rate Capacity for Multi-Cell Processing

The ergodic per-cell sum-rate capacity is given by [4]

$$C(P) = \frac{1}{L} E \left[\log_2 \left(\mathbf{I}_L + P \mathbf{H}_L \mathbf{H}_L^\dagger \right) \right] \quad (1)$$

where P is the transmit power of a single user, and the expectation is taken with respect to the fading coefficients \mathbf{H}_L . The matrix $\mathbf{H}_L \mathbf{H}_L^\dagger$ is an $L \times L$ matrix given by

$$\left[\mathbf{H}_L \mathbf{H}_L^\dagger \right]_{m,n} = \begin{cases} \mathbf{a}_m \mathbf{a}_m^\dagger + \mathbf{b}_m \mathbf{b}_m^\dagger & m = n \\ \mathbf{b}_m \mathbf{a}_n^\dagger & n = (m-1) \bmod L \\ \mathbf{a}_m \mathbf{b}_n^\dagger & n = (m+1) \bmod L \\ 0 & \text{otherwise} \end{cases} \quad (2)$$

The definition of spectrum efficiency, denoted as γ , is expressed as a function of the system average transmit E_b/N_0 [15]. Its value is solved by substituting

$$P = \frac{E_b}{K N_0} \gamma \quad (3)$$

in (1), and K is the number of users in a cell. The $\frac{E_b}{N_0}$ required for reliable communication is defined as

$$\frac{E_b}{N_{0 \min}} \triangleq \frac{\log_e 2}{C'(0)} \quad (4)$$

Then, the slope of the spectrum efficiency for low-SNR and high-SNR can be defined as

$$S_{\text{low}} \triangleq - \frac{2[C'(0)]^2}{C''(0)} = \lim_{\frac{E_b}{N_0} \rightarrow \frac{E_b}{N_{0 \min}}} \frac{10\gamma \log_{10} 2}{10 \log_{10} \frac{E_b}{N_0} - 10 \log_{10} \frac{E_b}{N_{0 \min}}} \quad (5)$$

$$S_{\text{high}} \triangleq \lim_{P \rightarrow \infty} PC'(P) = \lim_{\frac{E_b}{N_0} \rightarrow \infty} \frac{10\gamma \log_{10} 2}{10 \log_{10} \frac{E_b}{N_0}} \quad (6)$$

The upper and lower bounds for the fading channels are

Theorem 2. For $K \gg 1$, the average per-cell sum-rate capacity for Rayleigh fading satisfies

$$\log_{10}(1 + KP((1 - \varepsilon) \log_e K + 2)) \leq C(P) \leq \log_{10}(1 + 2KP \log_e K). \quad (7)$$

Theorem 3. The spectrum efficiency of channel for Rayleigh fading are characterized, for any number of BSs $M \geq 3$, by

$$S_{\text{low}} = 2; \quad S_{\text{high}} = 1; \quad \frac{(\log_e 2)^2}{2 \log_e K} \leq \frac{E_b}{N_{0 \min}} \leq \frac{(\log_e 2)^2}{(1 - \varepsilon) \log_e K + 2}. \quad (8)$$

In both theorems, the $\varepsilon = \Pr\{P > P_{\text{out}}\}$, indicating the possibilities that certain number of users passes a lower bound of the fading power that is needed to transmit. For example, the possibility that at least one of the users at a give cell cross the threshold is $1 - (1 - 1/K^{(1-\varepsilon)})^K$. If $K = 100$ and $\varepsilon = 0.1$, the possibility is 79.762%, and 99.997% for $\varepsilon = 0.5$. Refer to [11] for detail proofs of these two theorems.

C. Description of the System Model

Figure 1 illustrates an example deploying BSs in a 2D nested array manner. Every hexagon stands for a macrocell and the colored ones are deployed with actual BSs. It could be regarded as a simplified model of metroplex area containing both urban and suburb regions. Specifically, the sparse array is the lattice with blue color indexing $(x, 1)$, where $x \in [1, 14]$, and the dense array is the yellow hexagons in the middle.

As a result, its difference co-array is $\mathbf{N}^{(d)} = \begin{pmatrix} 1 & 0 \\ 0 & 1 \end{pmatrix}$, $\mathbf{P} = \begin{pmatrix} 2 & 0 \\ 0 & 3 \end{pmatrix}$, $N_1^{(s)} = 3$ and $N_2^{(s)} = 3$. Both the lattices towards

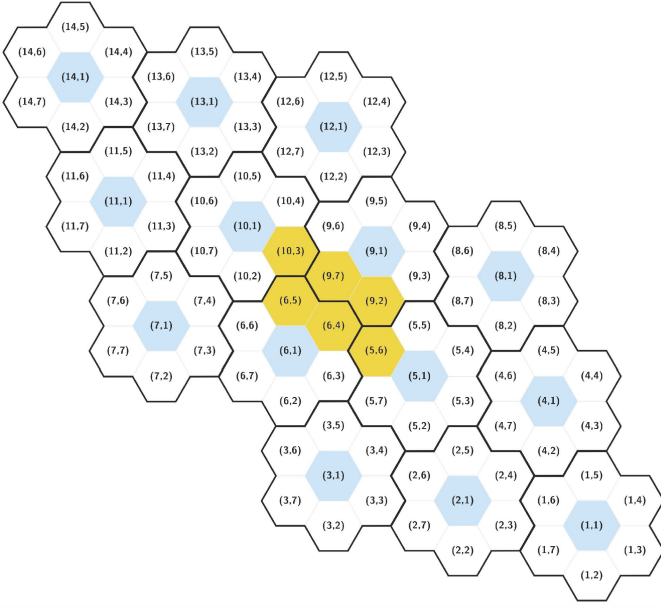


Fig. 1: Hexagonal cellular system model with BSs deployed in colored regions

upper left and lower right are regarded as the positive halves of the difference co-array, whose elements are given by

$$\left\{ \mathbf{N}^{(d)} [k_1, k_2]^T, - (p_1 - 1) \leq k_1 \leq (N_1^{(s)} - 1) p_1, \right. \\ \left. - (p_2 - 1) \leq k_2 \leq (N_2^{(s)} - 1) p_2 \right\}.$$

where p_1 and p_2 are the eigenvalues of the \mathbf{P} .

Based on the Theorem 1, we can conclude that the positive half of the co-array is a “filled” 2D array in the sense that $\text{SFPD}(\mathbf{N}^{(s)}, k_1, k_2)$ of the sparse array is completely filled by the dense array sensors for each k_1 and k_2 in the sparse array. From the Definition 3, we also know that the upper left “filled” lattice spans to a parallelogram grid of size $L = MN$, where $M = N_1^{(s)} N_1^{(d)}$ and $N = N_2^{(s)} N_2^{(d)}$.

Every cell has K users. The vector baseband representation of the signals received at the BSs is given as

$$\mathbf{y} = \mathbf{H}\mathbf{x} + \mathbf{n}, \quad (9)$$

where \mathbf{H} is the $L \times LK$ channel transfer matrix

$$\mathbf{H} = \begin{bmatrix} \mathbf{a}_0 & 0 & 0 & \dots & 0 & \mathbf{b}_0 \\ \mathbf{b}_1 & \mathbf{a}_1 & 0 & \dots & 0 & 0 \\ 0 & \mathbf{b}_2 & \mathbf{a}_2 & \dots & 0 & 0 \\ \vdots & \ddots & \ddots & \ddots & \vdots & \vdots \\ 0 & 0 & 0 & \dots & \mathbf{a}_{L-2} & 0 \\ 0 & 0 & 0 & \dots & \mathbf{b}_{L-1} & \mathbf{a}_{L-1} \end{bmatrix}, \quad (10)$$

in which \mathbf{a}_m and \mathbf{b}_m are $1 \times K$ row vectors denoting the channel coefficients experienced by the K users from the corresponding $\mathbf{N}^{(d)}$ and $\mathbf{N}^{(s)}$ BSs. It also assumes that the fading coefficients have complex values and are identical and independent distributed (i.i.d.) among different users.

The channel state information (CSI) is assumed available to the joint multicell BSs receivers only, and the channel coefficients are unknown for the transmitter. The transmitters know the channel statistics, which can be viewed as ergodic process. As a result, the users adjust their rates to this ergodic sum-rate capacity. It also assumes that the users cannot cooperate their transmissions, and use Gaussian codebooks so that the transmitted signal $\{\mathbf{x}\}_i^{LK}$ are i.i.d. zero-mean circularly symmetric Gaussian random variables with variance P . \mathbf{n} stands for the zero-mean circularly symmetric additive white Gaussian noise (AWGN) vector, and $E[\mathbf{n}\mathbf{n}^\dagger] = \mathbf{I}_L$, where \mathbf{I}_L is the $L \times L$ identity matrix. As a result, the power of transmission P is equal to the SNR value in the following derivation.

III. SUM-RATE CAPACITY OF NESTED DISTRIBUTED COOPERATIVE NETWORKS

A. Invariance in the Difference Co-Array

The concept of invariance is often referred in the algorithms for direction of arrival [16]. Specifically, it means that the array should be divisible into a number of identical subarrays which are the shifted copies of each other.

The maximum number of the subarrays is obtained by shifting the fundamental dense array with successive integer vectors. The improvement of rank is proportional to the number of dense arrays [17], while the degrees of freedom available after spacial smoothing is proportional to the size of the dense array. For constant elements to construct the array system, the best strategy is to make the rank equals to the size of dense array [18]. That is,

$$\mathbf{H}_{m,n}(i, j) = \mathbf{H}_{\mathbf{N}^{(d)}}[m \ n]^T, \quad (11)$$

where $-M + 1 \leq m \leq M - 1$, $-N + 1 \leq n \leq N - 1$, $0 \leq i < N_1^{(d)}$, $0 \leq j < N_2^{(d)}$.

The received signal by the subarray (m, n) is denoted as $\mathbf{y}_{m,n} = \mathbf{H}_{m,n}\mathbf{x} + \sigma_n^2 \mathbf{e}_{m,n}$, where the elements of $\mathbf{H}_{m,n}$ are given as

$$[\mathbf{H}_{m,n}]_{Nl+i,k} = \mathbf{H}_{\mathbf{N}^{(d)}} e^{j(\omega_{1k}(l-M+m) + \omega_{2k}(i-N+n))}$$

where $l = 0, \dots, M$, $i = 0, \dots, N$, $\omega_{1k} = 2\pi[\cos \theta_k \ \sin \theta_k] \mathbf{n}_1^{(d)}$, $\omega_{2k} = 2\pi[\cos \theta_k \ \sin \theta_k] \mathbf{n}_2^{(d)}$, and θ_k is the azimuthal angle of the source k . $\mathbf{N}^{(d)} = [\mathbf{n}_1^{(d)} \ \mathbf{n}_2^{(d)}]$. Then it is ready to derive that

$$\mathbf{y}_{m,n} = \mathbf{H}_{\mathbf{N}^{(d)}} \mathbf{\Lambda}_1^m \mathbf{\Lambda}_2^n \mathbf{x} + \sigma_n^2 \mathbf{e}_{m,n} \quad (12)$$

where $\mathbf{\Lambda}_1$ and $\mathbf{\Lambda}_2$ are $K \times K$ diagonal matrices with (i, i) th element given by $e^{j\omega_{1i}}$ and $e^{j\omega_{2i}}$, respectively. We can now define the autocorrelation of the received signal as

$$\begin{aligned} \mathbf{R}_{m,n} &\triangleq \mathbf{y}_{m,n} \mathbf{y}_{m,n}^\dagger \\ &= \mathbf{H}_{\mathbf{N}^{(d)}} \mathbf{\Lambda}_1^m \mathbf{\Lambda}_2^n \mathbf{x} \mathbf{x}^\dagger (\mathbf{\Lambda}_2^n)^\dagger (\mathbf{\Lambda}_1^m)^\dagger \mathbf{H}_{\mathbf{N}^{(d)}}^\dagger \\ &\quad + \sigma_n^4 \mathbf{e}_{m,n} \mathbf{e}_{m,n}^\dagger + \sigma_n^2 \mathbf{H}_{\mathbf{N}^{(d)}} \mathbf{\Lambda}_1^m \mathbf{\Lambda}_2^n \mathbf{x} \mathbf{e}_{m,n}^\dagger \\ &\quad + \sigma_n^2 \mathbf{e}_{m,n} \mathbf{x}^\dagger (\mathbf{\Lambda}_2^n)^\dagger (\mathbf{\Lambda}_1^m)^\dagger \mathbf{H}_{\mathbf{N}^{(d)}}^\dagger \end{aligned} \quad (13)$$

Taking the average of $\mathbf{R}_{m,n}$ over all (m,n) , we can define the rank-enhanced matrix

$$\hat{\mathbf{R}}^2 \triangleq \frac{1}{MN} \sum_{m=0}^M \sum_{n=0}^N \mathbf{R}_{m,n}, \quad (14)$$

since it provides the autocorrelations with the freedom of $N^{(s)}N^{(d)}$ BSs by using only $N^{(s)} + N^{(d)}$ BSs. Besides, it can also be shown that

$$\sum_{m=0}^M \sum_{n=0}^N \mathbf{\Lambda}_1^m \mathbf{\Lambda}_2^n \mathbf{x} \mathbf{x}^\dagger (\mathbf{\Lambda}_2^n)^\dagger (\mathbf{\Lambda}_1^m)^\dagger = \mathbf{R}_{xx} \mathbf{H}_{\mathbf{N}^{(s)}}^\dagger \mathbf{H}_{\mathbf{N}^{(d)}} \mathbf{R}_{xx} \quad (15)$$

$$\sum_{m=0}^M \sum_{n=0}^N \mathbf{\Lambda}_1^m \mathbf{\Lambda}_2^n \mathbf{x} \mathbf{e}_{m,n}^\dagger = \mathbf{R}_{xx} \mathbf{H}_{\mathbf{N}^{(s)}}^\dagger \quad (16)$$

$$\sum_{m=0}^M \sum_{n=0}^N \mathbf{e}_{m,n} \mathbf{e}_{m,n}^\dagger = \mathbf{I}_{M \times N} \quad (17)$$

Substituting the values from (15)-(17) in (14), we have

Proposition 1. *The covariance matrix of the signal received by a $M \times N$ array of BSs on the lattice $\tilde{\mathbf{N}}^{(d)}$ has the same form as $\hat{\mathbf{R}}^2$ where*

$$\begin{aligned} \hat{\mathbf{R}} &= \frac{1}{\sqrt{MN}} \left(\mathbf{H}_{\mathbf{N}^{(s)}} \mathbf{R}_{xx} \mathbf{H}_{\mathbf{N}^{(d)}}^\dagger + \sigma_n^2 \mathbf{I}_{M \times N} \right) \\ &= \frac{1}{\sqrt{MN}} \left(K P \mathbf{H}_{\mathbf{N}^{(s)}} \mathbf{H}_{\mathbf{N}^{(d)}}^\dagger + \sigma_n^2 \mathbf{I}_{M \times N} \right). \end{aligned} \quad (18)$$

Hence, the cluster of BSs has the degree of freedom as $O(N^{(s)}N^{(d)})$ with $O(N^{(s)} + N^{(d)})$ actual BSs.

B. Static AWGN Channel

Concerning the case of nonfading channels, all fading coefficients are equal to 1. Based on (2), it is easy to conclude that (1) depends only on the sum of the intra-cell transmit power. Hence, all transmission schemes with equal total intra-cell power achieve the same throughput.

The nonzero entries of $\mathbf{H}_L \mathbf{H}_L^\dagger$ derived from (2) are

$$[\mathbf{H}_L \mathbf{H}_L^\dagger]_{m,m} = \sum_{k=1}^K |a_{m,k}|^2 |b_{m,k}|^2, \quad (19)$$

$$[\mathbf{H}_L \mathbf{H}_L^\dagger]_{m,n} = \sum_{k=1}^K a_{n,k}^* b_{m,k}, \quad n = (m-1) \bmod L, \quad (20)$$

$$[\mathbf{H}_L \mathbf{H}_L^\dagger]_{m,n} = \sum_{k=1}^K a_{m,k} b_{n,k}^*, \quad n = (m+1) \bmod L. \quad (21)$$

As a result, the matrix $\mathbf{H}_L \mathbf{H}_L^\dagger$ is a circulant matrix with the nonzero row elements $\{K, 2K, K\}$. Based on the eigenvalues of the circulant matrices [19], we can have the following proposition.

Proposition 2. *The uplink average per-cell sum-rate capacity in the absence of fading is*

$$C(P) = \frac{1}{L} \sum_{l=0}^{L-1} \log_{10} \left(1 + 2KP \left(1 + \cos \left(2\pi \frac{l}{L} \right) \right) \right) \quad (22)$$

Substituting (22) into (4)-(6), we could have

Proposition 3. *The spectrum efficiency for uplink channel is characterized by*

$$\frac{E_b}{N_{0 \min}} = \frac{\log_e 2}{2}, \quad S_{\text{low}} = \frac{4}{3}, \quad S_{\text{high}} = 1. \quad (23)$$

C. Flat-Fading Channel

The channel fading coefficients are taken as i.i.d. random variables, and their statistics are denoted as

$$m_1 \triangleq E[a_{m,k}] = E[b_{m,k}], \quad (24)$$

$$m_2 \triangleq E[|a_{m,k}|^2] = E[|b_{m,k}|^2], \quad (25)$$

$$m_4 \triangleq E[|a_{m,k}|^4] = E[|b_{m,k}|^4], \quad (26)$$

$$\kappa \triangleq \frac{m_4}{m_2^2}, \quad \forall m, k, \quad (27)$$

to be the mean, second- and fourth-order moments and the kurtosis. The following contents assume that the users have similar large scale path losses to the BSs. Besides, given a rich scattering environment, the small-scale fading processes experienced by the users can be modeled as mutually i.i.d. random processes. For simplicity, it also assumes that all users are received with equal average power from the two BSs based on dense and sparse array, respectively. For the case that all users are simultaneously active, it also assumes that $K \gg 1$. Similarly to the derivation in [5], applying the Strong Law of Large Number (SLLN) to K while keeping the total per-cell transmit power KP constant, the diagonal entries of (2) can be represented using (24)-(27)

$$\lim_{K \rightarrow \infty} \left[\frac{1}{K} \mathbf{H}_L \mathbf{H}_L^\dagger \right]_{m,m} = 2E[|a_{m,k}|^2] = 2m_2 \quad (28)$$

$$\lim_{K \rightarrow \infty} \left[\frac{1}{K} \mathbf{H}_L \mathbf{H}_L^\dagger \right]_{m,n} = |E[a_{m,k}]|^2 = |m_1|^2 \quad (29)$$

$$\lim_{K \rightarrow \infty} \left[\frac{1}{K} \mathbf{H}_L \mathbf{H}_L^\dagger \right]_{n,m} = |E[a_{m,k}]|^2 = |m_1|^2 \quad (30)$$

Substituting (28)-(30) to (1), we could have

Proposition 4. *The average per-cell sum-rate capacity while the transmission experiencing Rayleigh fading is*

$$\begin{aligned} C(P) &= \\ &= \frac{1}{L} \sum_{l=0}^{L-1} \log_{10} \left(1 + 2KP \left(m_2 + |m_1|^2 \cos \left(2\pi \frac{l}{L} \right) \right) \right). \end{aligned} \quad (31)$$

Comparing the capacity (31) with (22), we can see that the presence of fading enhance the performance in terms of the average per-cell sum-rate capacity. This is because the independence of the two fading processes affecting the signal of each user, as observed by the two receiving BSs. Furthermore, by applying (31) to (4)-(6), we could have

Proposition 5. *For a general fading distribution, $K \gg 1$, and $\forall L \geq 3$, the average per-cell sum-rate capacity is*

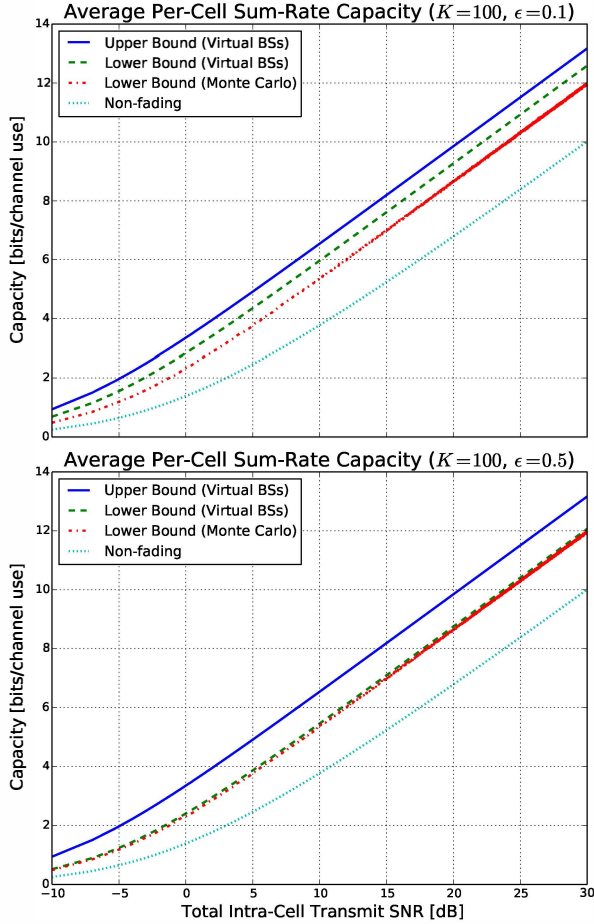


Fig. 2: Comparison of Average Per-Cell Sum-Rate Capacity for $K = 100$, and $\varepsilon = 0.1$ or $\varepsilon = 0.5$

characterized by

$$\frac{E_b}{N_{0\min}} = \frac{\log_e 2}{2m_2}, \quad S_{\text{low}} = \frac{2}{\frac{\kappa}{2K} + \frac{|m_1|^4}{2m_2} + 1}, \quad S_{\text{high}} = 1. \quad (32)$$

Specifically for Rayleigh fading, the expressions are

$$\frac{E_b}{N_{0\min}} = \frac{\log_e 2}{2}, \quad S_{\text{low}} = 2, \quad S_{\text{high}} = 1. \quad (33)$$

In the low-SNR region, the minimum transmit E_b/N_0 that enables reliable communications is the same for either intra-cell TDMA, which means that only a single user simultaneously in each cell transmits for a fraction $1/K$ of time with the power P , or in the wideband scenario. It is also identical with or without fading. However, in the presence of Rayleigh fading, employing the wideband scheme with more than two simultaneously active users per cell produces a higher low-SNR slope, and hence a higher spectrum efficiency, as compared to the result for nonfading channels.

IV. NUMERICAL RESULTS

Figure 2 shows the values of channel capacities in no fading (22) and Rayleigh fading (31) channels as a function of the

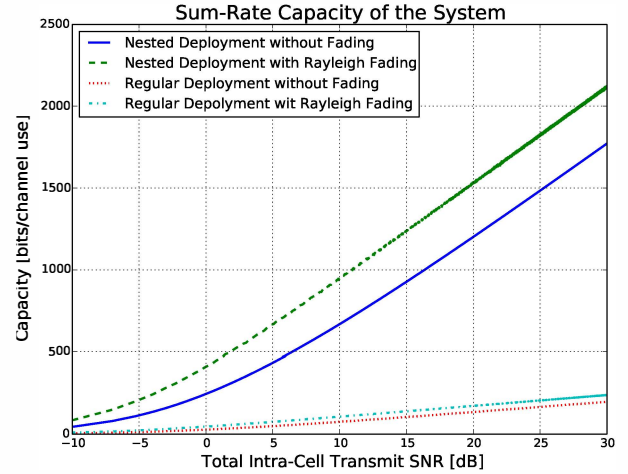


Fig. 3: Comparison of Sum-Rate Capacity for Nested and Regular Deployment

total intra-cell transmit power. For comparison, it also includes the analytical derived upper and lower bounds (7) with $K = 100$ users per cell. The upper figure shows the lower bound for $\varepsilon = 0.1$, while the lower figure shows the lower bound for $\varepsilon = 0.5$. Comparing the results of nonfading channels with those of Rayleigh-fading channels, it is obvious that the fading has a positive impact on system performances. Besides, the Monte Carlo simulations have a good match to the analytical lower bound. Furthermore, given a certain number of users in a cell, a higher value of ε implies that more users are likely to experience threshold crossing fading coefficients, so the lower bound, which is derived based on the SLLN, yields a better approximation. This phenomenon is able to be observed by comparing the two figures in Figure 2, in which the results of Monte Carlo simulations are closer to the analytical lower bound with $\varepsilon = 0.5$ than it is with $\varepsilon = 0.1$.

Figure 3 shows the comparison of sum-rate capacity in the system point of view. The regular deployment stands for the deploying BSs in a common hexagon manner, while the nested deployment is elaborated in the previous contents. Both deployments involve the same number of BSs. Based on the figure, the capacity improvement is substantial. Specifically, the capacity increases by about eight times for non-fading channel, and seven times for the Rayleigh-fading channel.

Figure 4 shows the corresponding per-cell spectrum efficiency results, plotted as a function of the system average transmit E_b/N_0 . The beneficial effect of fading on system performance is again clearly demonstrated, and a good match to the low-SNR regime characterization of Proposition 5 is observed.

V. CONCLUDING DISCUSSION

The feasibility and characteristics for the nested distributed cellular network are discussed in this paper based on a traditional hexagonal multi-cell model. The model assumes a modified version of soft-handoff scenario, in which each user simultaneously communicates with two BSs, and at least

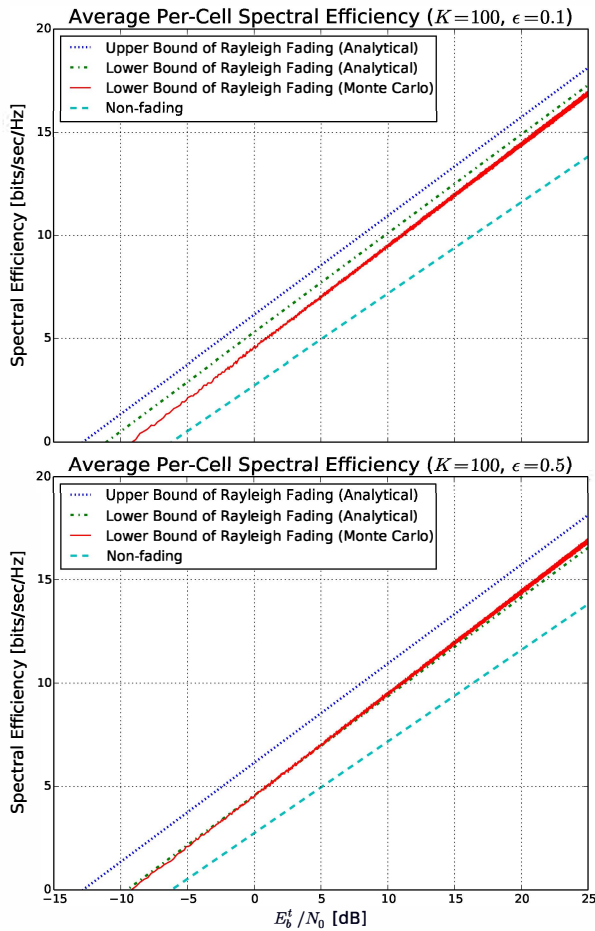


Fig. 4: Average Per-Cell spectrum efficiency for $K = 100$, and $\varepsilon = 0.1$ or $\varepsilon = 0.5$

one of them is the BS from the dense array. Both the non-fading and Rayleigh fading channels are analyzed in terms of the average per-cell sum-rate capacity and spectrum efficiency. It shows that the invariant of difference co-array is valid to analyze the covariance of channel fading coefficients, which plays an important role to derive the cell capacity. The numeric results also support the correctness of the propositions.

A key insight of the present work is that by carefully deploying and scheduling communication between users and different BSs, the cluster of the BSs is able to achieve a much higher capacity compared to the simple collaboration among BSs. On the other hand, there are many open questions in this direction of research, including detailed power allocation and beamforming for the combination of dense array and sparse array, the interference analysis when this nested distributed cellular network is put into a system at large, and the relation between the uplink and downlink channels.

ACKNOWLEDGMENT

This work was supported in part by U.S. National Science Foundation under Grants CNS-1247848, CNS-1116749, CNS-0964713, U.S. Office of Naval Research under Grants N00014-

13-1-0043, N00014-11-1-0865, and National Science Foundation of China (NSFC) under Grant 61372097.

REFERENCES

- [1] J.G. Andrews, H. Claussen, M. Dohler, S. Rangan, and M.C. Reed, "Femtocells: Past, present, and future," *IEEE J. Sel. Areas Commun.*, vol. 30, no. 3, pp. 497-508, Apr. 2012.
- [2] A. Lozano, R.W. Heath, and J.G. Andrews, "Fundamental limits of cooperation," *IEEE Trans. Information Theory*, vol. 59, no. 9, pp. 5213-5226, Sep. 2013.
- [3] H. Dai, A.F. Molisch, and H.V. Poor, "Downlink capacity of interference-limited MIMO systems with joint detection," *IEEE Trans. Wireless Communications*, vol. 3, no. 2, pp. 442-453, Mar. 2004.
- [4] A.D. Wyner, "Shannon-theoretic approach to a Gaussian cellular multiple-access channel," *IEEE Trans. Information Theory*, vol. 40, no. 6, pp. 1713-1727, Nov. 1994.
- [5] O. Somekh and S. Shamai, "Shannon-theoretic approach to a Gaussian cellular multiple-access channel with fading," *IEEE Trans. Information Theory*, vol. 46, no. 4, pp. 1401-1425, Jul. 2000.
- [6] S.A. Jafar and A.J. Goldsmith, "Transmitter optimization for multiple antenna cellular systems," in *Proc. IEEE Int. Symp. Information Theory*, Lausanne, Switzerland, p. 50, Jun. 2002.
- [7] W. Yu, "Uplink-downlink duality via minimax duality," *IEEE Trans. Information Theory*, vol. 52, no. 2, pp. 361-374, Feb. 2006.
- [8] M. Costa, "Writing on dirty paper," *IEEE Trans. Information Theory*, no. 3, vol. 29, pp. 439-441, May 1983.
- [9] G. Caire and S. Shamai, "On the achievable throughput of a multiple-antenna Gaussian broadcast channel," *IEEE Trans. Information Theory*, vol. 49, no. 7, pp. 1691-1706, Jul. 2003.
- [10] M. Karakayali, G. Foschini and R. Valenzuela, "Network coordination for spectrally efficient communications in cellular systems," *IEEE Trans. Wireless Communications*, vol. 13, no. 4, pp. 56-61, Aug. 2006.
- [11] O. Somekh, B.M. Zaidel, and S. Shamai, "Sum rate characterization of joint multiple cell-site processing," *IEEE Trans. Information Theory*, vol. 53, no. 12, pp. 4473-4497, Dec. 2007.
- [12] O. Simeone, O. Somekh, and S. Shamai, "Local base station cooperation via finite-capacity links for the uplink of linear cellular networks," *IEEE Trans. Info. Theory*, vol. 55, no. 1, pp. 190-204, Jan. 2009.
- [13] P. Pal and P.P. Vaidyanathan, "Nested arrays: A novel approach to array processing with enhanced degrees of freedom," *IEEE Trans. Signal Processing*, pp. 4167-4181, Aug. 2010.
- [14] P. Pal and P.P. Vaidyanathan, "Nested arrays in two dimensions, part I: Geometrical considerations," *IEEE Trans. Signal Processing*, vol. 60, no. 9, pp. 4694-4705, Sep. 2012.
- [15] V. Sergio, "spectrum efficiency in the wideband regime," *IEEE Trans. Information Theory*, vol. 48, no. 6, pp. 1319-1343, Jun. 2002.
- [16] R. Roy and T. Kailath, "ESPRIT-estimation of signal parameters via rotational invariance techniques," *IEEE Trans. Acoust., Speech Signal Process.*, vol. 37, no. 7, pp. 984-995, Jul. 1989.
- [17] S.U. Pillai and B.H. Kwon, "Forward/backward spatial smoothing techniques for coherent signal identification," *IEEE Trans. Acoust., Speech Signal Process.*, vol. 37, no. 1, pp. 8-15, Jan. 1989.
- [18] P. Pal and P.P. Vaidyanathan, "Nested arrays in two dimensions, Part II: Application in two dimensional array processing," *IEEE Trans. Signal Processing*, vol. 60, no. 9 pp. 4706-4718, Sep 2012.
- [19] R.M. Gray, "On the asymptotic eigenvalue distribution of Toeplitz matrices," *IEEE Trans. Information Theory*, vol. 18, no. 6, pp. 725-730, Nov. 1972.